Application of Adaptive Control Theory to On-Line GTA Weld Geometry Regulation

A. Suzuki
Research Assistant
(now with Konica USA).

D. E. Hardt
Leaders for Manufacturing Professor
of Mechanical Engineering,
Laboratory for Manufacturing & Productivity.

L. Valavani
Associate Professor,
Department of Aeronautics and Astronautics.

Massachusetts Institute of Technology,
Cambridge, Mass. 02139

This study addresses the uses of adaptive schemes for on-line control of backbead width in the Gas Tungsten Arc (GTA) welding process. Open-loop tests using a step input current confirm the validity of a nominal first order process model. However, the time constant and gain prove highly dependent upon welding conditions including torch speed, arc length, material thickness, and other material properties. Accordingly, a need exists for adaptive controllers that can compensate for these process nonlinearities. The performance of two adaptive controllers is evaluated: Narendra and Lin's Model-Referenced Adaptive Control (MRAC/NL), and Self-Tuning Control with Pole Placement (STC/PP). The addition of a quadratic term to the adaption mechanisms of MRAC/NL is proposed and preliminary simulations and experiments clearly demonstrate the stabilizing effect of this added term. The main experiments compare the performance of the modified MRAC/NL controller and the STC/PP controller with each other and with linear PI controller and the STC/PP controller with each other and with linear PI controller under four experimental conditions: first, where welding conditions are nominal; second, when conditions are disturbed by a step-wise increase in the torch velocity, and third, when conditions are disturbed by a step-wise increase in material thickness. In each case the experimental demonstrates the superiority of the adaptive controllers over the linear PI controller. However, the STC/PP controller exhibits high frequency control action in response to severe disturbances of material thickness and the parameter estimates it generates drift during steady-state operations. The MRAC/NL controller proves more robust under these circumstances. Analysis demonstrates that the superior performance of the MRAC/NL is due both to the inherent normalizing effect of the quadratic feedback terms and to the noise filtering properties of the adaptive mechanism.

Introduction

This paper examines the use of adaptive control for the real-time control of full penetration Gas Tungsten Arc (GTA) welding. In this type of welding, backbead geometry is a major determinant of final weld quality. Hardt et al. (1985) show that a simple heat balance analysis of the idealized weld pool leads to a dynamic relationship between current input and the backbead width output by a simple first order model. They also demonstrate that the time constant and the process gain are a function of weld conditions such as preheat temperature, welding speed and material thickness, as well as material thermal properties. Ample literature demonstrates the dependence of the process characteristics upon these operating conditions (Mills, (1979); Walsh and Savage, (1985); Leinonen, (1985); and Kureishi, (1980). For instance, in Leinonen, (1985), the cast-to-cast variations in GTA weld penetration of stainless steel are shown to be caused by the variations of CaO content of the workpiece. Vroman and Brandt (1976) and Smith (1974) attempted simple closed-loop bead width control, but because of these varying parameters and nonlinearity in the process, the linear fixed parameter control strategy has not always proved satisfactory. Hardt et al. (1985) and Oshima (1987) attest to the need for an adaptive control scheme. Accordingly, adaptive control is a potential candidate for the real time control of weld quality.

By 1980 considerable theoretical progress had been made in the field of adaptive control, resulting in the analysis and design of Model-Referenced Adaptive Control (MRAC) (Monopoli, 1974; Narendra and Valavani, 1978; Landau, 1979, Goodwin et al. 1980; Egardt, 1980; and Narendra and Lin, 1980) and Self-Tuning Control (STC) systems (Astrom and Wittenmark, (1980).

However, the number of experimental studies of adaptive control has been small compared to the theoretical progress

Contributed by the Dynamic Systems and Control Division for publication in the JOURNAL OF DYNAMIC SYSTEMS, MEASUREMENT, AND CONTROL. Manuscript received by the Dynamic Systems and Control Division July 9, 1989; revised manuscript received November 15, 1989. Associate Editor: A. G. Ulsoy.

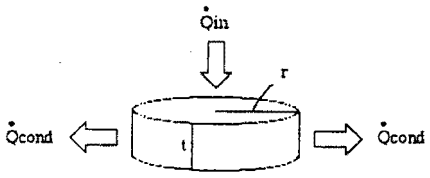

Fig. 1 Idealized weld pool geometry for heat balance

that has been made. These studies are typically concerned with the adaptive control of chemical processes (Clarke and Gawthrop, 1981; Kershenbaum and Fortescue, 1981, heat exchangers, (Kurz et al., 1980), paper machines. (Cegrell and Hedquist 1975), mechanical drive systems (Finney et al., 1985), and rolling processes (Desrochers, 1981). Each experimenter chooses his own adaptive control scheme and pays great attention to implementation. It is believed that these ad-hoc experiments serve to enhance understanding and evaluation of the adaptive algorithm on the one hand and result in improved yet safe operation of large classes of systems, on the other.

The purpose of the present paper is to demonstrate the utility of adaptive control schemes over the conventional PI controller in the context of the GTA welding process and to compare and analyze the performance of two classes of adaptive controllers: Model Reference Adaptive (MRAC) and Self-Tuning (STC).

Process Dynamics for GTA Welding

A basic process model for GTA full penetration weld control has been derived in Hardt et al. (1985) and is reviewed below. Consider the idealized cylindrical weld pool shown in Fig. 1. Assuming that the pool is isothermal and that the pool phase change is the dominant dynamics, then the heat balance for the system is

$$Q_{in} = Q_{cond} + \rho h \frac{dV}{dt} \tag{1}$$

where Q_{in} is the heat input to the pool. Q_{cond} is the heat conducted through the pool, and ρ, h, and dV/dt are the density, heat of fusion and rate of change of the pool volume, respectively. Further, the conduction term is approximated by

$$Q_{cond} = 2\pi t\, k\, r \frac{d\Theta}{dr} \tag{2}$$

where k is the thermal conductivity of the weld and $d\Theta/dr$ represents a radial temperature gradient. From these two equations, we get the relationship between heat input and the pool radius:

$$(\rho h 2\pi t\, r)\frac{dr}{dt} + \left(k\, 2\pi t \frac{d\Theta}{dr}\right) r = Q_{in} \tag{3}$$

or

$$C(r, t)dr/dt + G(k, t, d\Theta/dr)\, r = Q_{in} \tag{4}$$

Further, the heat input is given by

$$Q_{in} = \eta E I \tag{5}$$

where η is an arc efficiency, E is an arc potential, and I is a welding current. Assuming for the moment that C and G are constant, then we get the first-order transfer function:

$$\frac{R(S)}{I(S)}e = \frac{K}{\tau s + 1} \tag{6}$$

where

$$K = \frac{\eta E}{G(k,t,d\Theta/dr)} \tag{7}$$

and

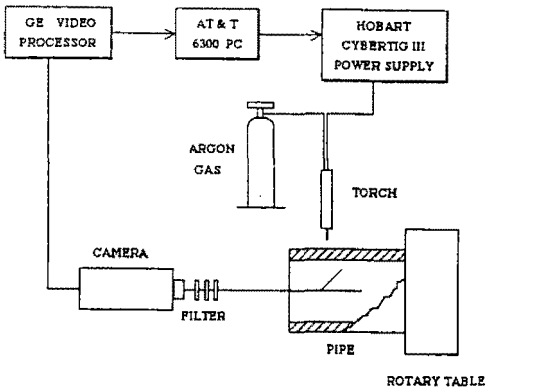

Fig. 2 Schematic representation of the GTA welding setup

$$\tau = \frac{C(r,t)}{G(k,t,d\Theta/dr)} \tag{8}$$

The implication of this simple model is that, although the dynamic behavior of the process is essentially first order, it is in fact a nonlinear process in that the time constant is a function of radius and that the process variables such as thickness and temperature gradient affect both time constant and system gain. This dependence of the process parameters on the welding condition is examined next in a series of open-loop step response tests.

Experimental Setup

A series of experiments were performed to enhance understanding of the bead width dynamics and the examine quantitatively the effect of typical welding disturbances. Figure 2 shows the schematic representation is conducted on the 304 stainless steel pipe of 0.109 in thickness, 6 5/8 O.D. and 12 in. Length.The pipe is held in a chuck mounted on the rotary table driven by the computer controller D.C. servo motor with high bandwidth compared to the process. A Heliarc HG-20 water-cooled torch with a 0.094 in. diameter 2 percent thoriated tungsten electrode of 3 in. length and a 60 degree include angle is mounted on a stand. High purity Argon gas is used as shielding gas at 55 cfg. The power supply unit is a Hobart Cybertig III GTA welding supply with a bandwidth of 0-1 kHz for operation of up to 150 Amps.

A General Electric (GE) Optomation Instrument Vision System processes the image sent from a GE CID camera viewing the backside of the pipe through a mirror and a series of optical filters. The system is capable of computing various geometrical features of detected images using the GE interpretive Optomation language. A program to find the maximum width was developed by drawing a rectangle circumscribing the detected pool image. This program can run at up to 10 Hz. Several combinations of optical filters were tried to check their ability to detect the onset of full penetration and its was found that the combination of neutral density, infra-red filter, and green filters gives the best agreement measurement and the actual bead width. This result also agrees with the result in Bennett and Smith [1976] that the narrow band filter of 0.45–0.55 μm provides the maximum detector sensitivity to the molten pool. (The CID camera has quite a wide spectral response of 0.4–0.95 μm (GE Optomation II Manual, 1981)).

The computed width is sent from the GE instrument to an AT&T PC 6300 microcomputer as an 8 bit number, while the microcomputer sends a voltage command ranging from O V to 10 V through a digital to analog converter to the power supply corresponding to 0 to 200 Amps.

Open-Loop Step Response

The effects of the various welding conditions on the process

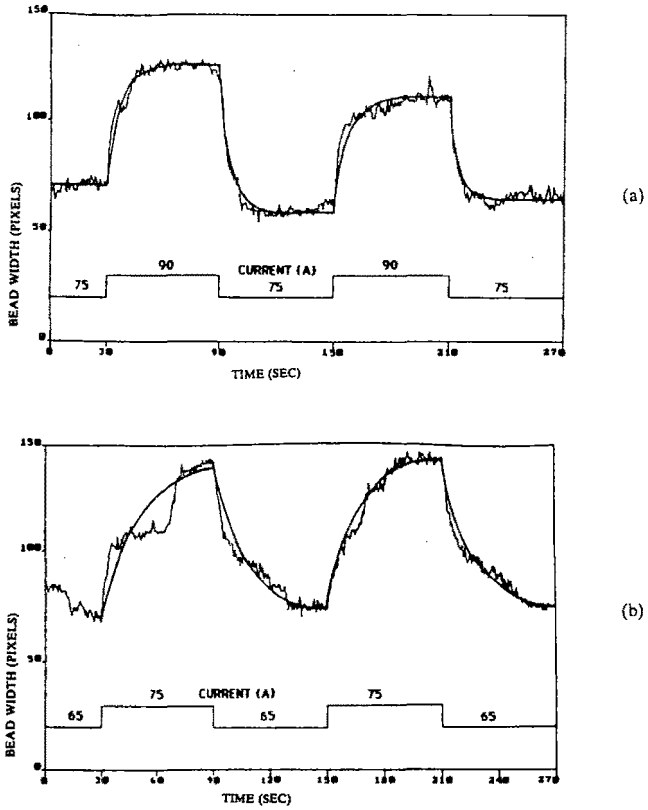

Fig. 3(*a*) Open-loop step response with arc length = 0.125 in., velocity = 3.2 in/min and current = 75A/90A; (*b*) open-loop step response with arc length = 0.125 in., velocity = 1.6 in/min and current = 65A/75A

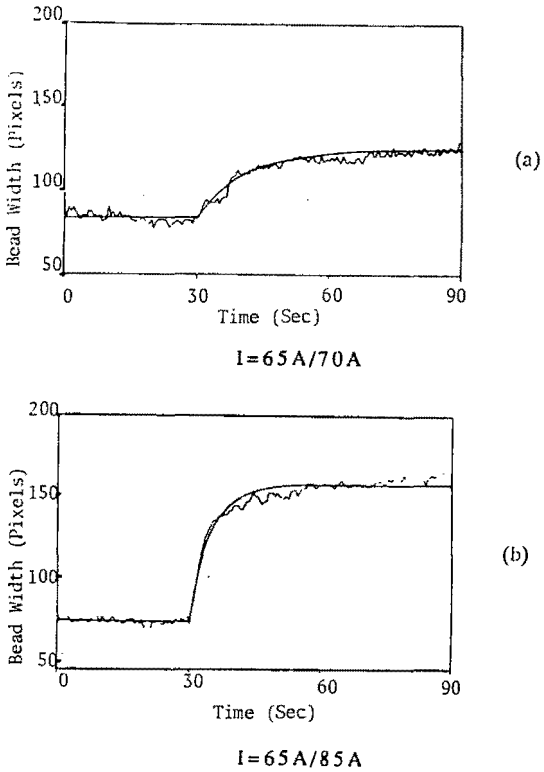

Fig. 4 Effects of input current magnitude on open-loop response (arc length = 0.08 in., torch velocity = 1.6 in/min)

dynamics were examined by means of open-loop step response tests. In each case the weld is first brought to steady state and then steps in either process inputs (torch velocity, arc voltage or arc current) or boundary conditions (material thickness) are applied.

The basic current input step response of the system is shown in Fig. 3. From this plot it can be observed that the time and gain vary with the direction of the step (i.e., heating or cooling of bead) and with time (progressive pre-heating of the weldment). Comparison of Fig. 3(*a*) and 3(*b*) illustrates as well the strong effect of velocity on time response. Indeed, in some cases, a time constant variation of 2-3 times was observed for negative versus positive steps.

In Fig. 4, the effect of input magnitude is shown. Clearly the settling time of the 5 ampere step of Fig. 4(*a*) is 2-3 times longer than the settling time of 4(*b*) where a 20 amp step is followed. This process clearly exhibits rapid and large magnitude parametric charges when viewed as a linear, non-stationary plant. A first-order model was fit to the data (using a least squares method), which gives the approximate time constant and the gain for each step in each case.

Finally, the response of the process to an increase in plate thickness was examined using the pipe shown in Fig. 5. (It should be noted that because of imperfect rolling of the attached plates, there is an air gap between the two materials in some regions. Moreover, the arc length is shortened over the attached sheet due to to geometry. Therefore, this preparation is not a pure thickness change but the combination of all these elements.) In Fig. 6, a step input from 90A to 100A is given about halfway on the thick part. The effect of thickness is shown both by both the decrease in width as thickness increases and the relatively slow step response observed. It is also noticed that there is a significant change in operating points. Towards the end, the input was shut off, since 100A of current would easily melt through the original pipe wall.

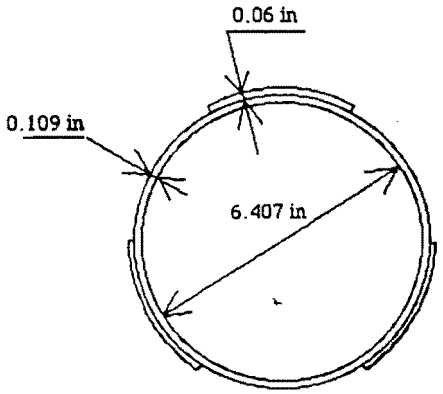

Fig. 5 Thickness change disturbance: three pieces of 3 in. × 12 in. × 0.06 in. SUS 304 plates are attached on the pipe surface

Adaptive Controller for GTA Welding

Weld Bead Width Control. The objective of backbead width control is to regulate the width to constant values as various disturbances occur. Because of the inherently nonstationary process dynamics, a set of adaptive controllers will be examined for this control task. Later, experiments will compare these with a conventional PI control loop.

As shown above, the GTA welding process can be modeled by a first-order system with a time constant and gain that are sensitive to the welding conditions and material properties. Therefore, the plant model used for the controller design is:

$$G(s) = \frac{K_p}{\tau_p s + 1} \tag{9}$$

or in its ZOH equivalence form:

$$G(z) = \frac{b}{z + a} \tag{10}$$

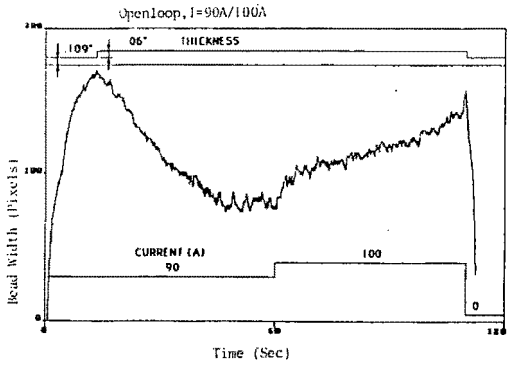

Fig. 6 Thickness disturbance with a step input at the middle (I = 90A→100A), (arc length = 0.08 in/0.14 in, velocity = 1.6 in/min)

where

$$a = -e^{-(T_s/s_p)} \tag{11}$$

$$b = K_p(1-a) \tag{12}$$

T_s = sample time

In what follows, two types of adaptive controllers are designed: the STC combined with pole placement (STC/PP) and the MRAC of Narendra and Lin (MRAC/NL) (Narendra and Lin, 1980). Although the STC and MRAC are based on different design philosophies, that is, the former is a "heuristic" combination of estimation and control whereas the latter is based on stability considerations, it has been shown that the STC can also be derived from stability based approach and vice-versa (Egardt, 1980). Nonetheless, the resulting parameterizations in the algorithms are different as in the overall performance of the two systems. Therefore, it is quite meaningful to test these two representative algorithms from each category.

Among other discrete MRACs the algorithm of Goodwin et al. (1980) is applicable but, since it relies on the dead-beat control scheme, it is not very favorable under the presence of modeling error and output noise. Doumanidis and Hardt (1988), however, applied this algorithm with good success to control the thermal properties of the Gas Metal Arc Welding process. This algorithm was chosen because it handles multiple input and multiple output systems well, and because the thermal system is quite slow. However, to avoid high frequency action caused by the dead-beat control, it was necessary to augment the adaptive controller with an outer PI control loop. This was possible since the open-loop and the desired closed-loop system bandwidth with relatively small. (Closed-loop settling time was about $15 \approx 30$ seconds.)

STC With Pole Placement (STC/PP). The general design procedure for this scheme has been summarized in Astrom and Wittenmark (1984). One of the merits of this algorithm is that it can incorporate an integrator so as to achieve high loop gain at low frequencies. The controller structure is shown in Fig. 7.

$$U(z) = \frac{T(z)}{R(z)} r(z) - \frac{S(z)}{R(z)} Y(z) \tag{13}$$

The polynomials $R(z)$, $T(z)$, and $S(z)$ for the welding process are designed as follows:

$$R(z) = b(z-1) \tag{14}$$

$$T(z) = b_m(z+\alpha) \tag{15}$$

$$S(z) = S_0 z + S_1 \tag{16}$$

where

$$S_0 = a_m - a + \alpha + 1 \tag{17}$$

$$S_1 = a_m\alpha + a \tag{18}$$

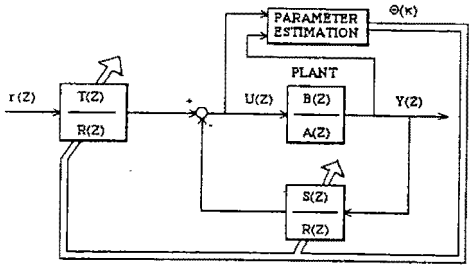

Fig. 7 STC/PP controller

α = "observer" pole

and a_m and b_m are defined by the desired model transfer function:

$$G_m(z) = \frac{b_m}{z+a_m} \tag{19}$$

Note the integrator in equation (14).

The controller is implemented by the following recursive formula:

$$U_k = U_{k-1} + \frac{b_m}{b}(r_k + \alpha r_{k-1}) - \frac{s_0}{b}\left(y_k + \frac{s_1}{s_0} y_{k-1}\right) \tag{20}$$

Since a and b are unknown, they are replaced by their estimates a_k and b_k which are updated by the recursive least squares method:

$$\theta_k = \theta_{k-1} + P_k\phi_k(y_k - \theta_{k-1}{}^T\phi_k) \tag{21}$$

$$\theta_T = [ab] \tag{22}$$

$$\phi_k = [-y_{k-1}u_{k-1}]^T \tag{23}$$

$$P_k = \frac{1}{\lambda} P_{k-1} - \frac{P_{k-1}\phi_k\phi_k{}^T P_{k-1}}{\lambda + \phi_k{}^T P_{k-1}\phi_k} \tag{24}$$

where

$\lambda \in [0, 1]$ is called for forgetting factor, and P is the covariance matrix.

Note that the closed-loop system is expressed by:

$$\frac{Y(z)}{R(z)} = \frac{B(z)T(z)}{A(z)R(z) + B(z)S(z)} \tag{25}$$

If a and b are known or $a_k = a$, $b_k = b$, then closed-loop pole located at $z = -a_m$ and $z = -\alpha$ and the second pole is canceled by the closed-loop zero at $z = -\alpha$, thus achieving the desired transfer function. If not (which is always the case), the closed-loop poles will be located somewhere in the vicinity of $z = -a_m$ and $z = -\alpha$, at best, and the second pole is not canceled by the zero, thereby affecting the closed-loop response if the poles deviate considerably. Therefore, the α or an "observer" pole should be neither too slow nor too fast as compared to the model pole. Thus, $\alpha = a_m$ has been chosen in all the experiments. The consequences of other important design parameters are discussed below.

MRAC of Narendra and Lin (MRAC/NL). In what follows we maintain the same notation as in Narendra and Lin (1980) for convenience. However, during the course of this research, it was found that a change in the algorithms was necessary to enhance nominal stability. To illustrate this fact, this algorithm will be discussed in greater detail.

The plant with input $u(k)$ and output $y_p(k)$ and the reference model with input $r(k)$ and output $y_m(k)$ are represented by the following transfer functions:

$$G_p(z) = k_p \frac{B_p(z)}{A_p(z)} \tag{26}$$

$$G_m(z) = k_m \frac{B_m(z)}{A_m(z)} \tag{27}$$

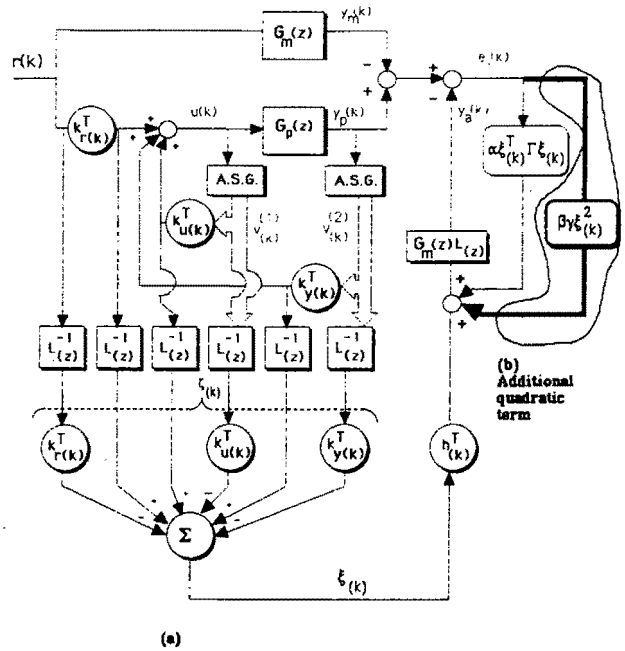

Fig. 8 Controller structure of MRAC/NL algorithm for n-$m \geq 1$ and unknown gain k_p;
(*a*) standard configuration;
(*b*) with new quadratic term

where $B_p(z)$, $B_m(z)$ and $A_m(z)$ are monic, stable polynomials of degree m, M, and n, respectively, $A_p(z)$ is a monic polynomial of degree n; k_p and k_m are constant (high frequency) gains. The algorithm described in Narendra and Lin (1980) assumes, for simplicity, that the plant gain is known, i.e., $k_p = k_m$; a rigorous proof of stability is also given. The controller structure in that case is depicted in Fig. 8, where the vector $\mathbf{K}_y(k)$ and $\mathbf{K}_u(k)$ are the adjustable controller gains, $\mathbf{v}^{(1)}(k)$ and $\mathbf{v}^{(2)}(k)$ are the auxiliary plant state variables, ASG represents and Auxiliary Signal Generator filter of order $n-1$ and $L^{-1}(z)$ is a strictly proper minimum phase transfer function, which is chosen such that $G_m(z)L(z)$ is strictly positive real.

The scalar control input to the plant is

$$u(k) = \phi(k) w(k) \tag{28}$$

$$\phi(k) - [K_u(k) K_y(k)]^T \tag{29}$$

$$w^T(k) = [\mathbf{v}_{(k)}^{(1)T} \mathbf{v}_{(k)}^{(2)T}] \tag{30}$$

The output error is defined by

$$e(k) = y_p(k) - y_m(k) \tag{31}$$

and the augmented error is defined by

$$y_a(k) = G_m(z)L(z)\,(-\xi(k) - \alpha\zeta^T(k)\Gamma\zeta(k)e_1(k)) \tag{32}$$

and

$$e_1(k) = e(k) + y_a(k) \tag{33}$$

where

$$\xi(k) = L^{-1}(z)\phi(k)^T w(k) - \phi(k)^T L^{-1}(z) w(k) \tag{34}$$

$$\zeta(k) = L^{-1}(z) w(k) \tag{35}$$

α and Γ are constant adaptation gains.

The following adaptive law has been shown in Narendra and Lin (1980) to result in $\lim_{k\to\infty} e_1(k) = 0$:

$$\phi(k+1) = \phi(k) - \Gamma e_1(k)\zeta(k) \tag{36}$$

where

$$\Gamma = \Gamma^T > 0 \tag{37}$$

$$\alpha > \frac{1}{2} \tag{38}$$

The proof of boundedness of $y_p(k)$ and $y_m(k)$ is given in Narendra and Lin (1980).

If k_p is unknown, as in most cases, an additional adjustable parameter $h(k)$ must be introduced, as was stated in the original paper. However, the introduction of $h(k)$ requires another quadratic feedback term in the augmented error generation in order to guarantee even nominal stability; this was overlooked in Rohrs (1982). We have completed this algorithm with this additional quadratic term ($\beta\gamma\xi^2_{(k)}$) illustrated in Fig. 8.

The complete adaptive law for this case given by

$$\phi(k+1) = \phi(k) - \Gamma e_1(k)\zeta(k) \tag{39}$$

and

$$h(k+1) = h(k) + \gamma e_1(k)\xi(k) \tag{40}$$

where $e_1(k)$, $\zeta(k)$, and $\xi(k)$ are defined by Equations (33), (35), (34), respectively and other variables are defined by:

$$y_a(k) = G_m(z)L(z)\,(-h(k)\xi(k) - \alpha\zeta^T(k)\Gamma\zeta(k)e_1(k) - \beta\gamma\xi^2(k)e_1(k)) \tag{41}$$

$$\phi(k) = [K_r^T(k), K_u^T(k), K_y^T(k)] \tag{42}$$

$$w_T(k) = [r(k), \mathbf{v}_{(k)}^{(1)T}, \mathbf{v}_{(k)}^{(2)T}] \tag{43}$$

$$\gamma > 0 \tag{44}$$

$$\alpha > \frac{1}{2}\frac{k_p}{k_m} \tag{45}$$

$$\beta > \frac{1}{2} \tag{46}$$

and Γ is defined by equation (37).

The requirement for the additional feedback term is made clear by examining the Lyapunov function candidate and its discrete time difference as summarized below. The error equation for the system yields, after some algebra:

$$e_1(k) = \{G_m(z)L(z)\}\{\psi^T(k) - k_0^*\alpha\zeta^T(k)\Gamma\zeta(k)e_1(k) - k_0^* h(k)\xi(k) - k_0^*\beta\gamma\xi^2(k)e_1(k)\} \tag{47}$$

where

$$\psi(k) = \phi(k) - \phi^* \tag{48}$$

$$h(k) = h(k) - h^* \tag{49}$$

and

$$k_0^* = \frac{k_m}{k_p} \tag{50}$$

ϕ^* and h^* are constant parameters such that when $\phi(k) = \phi^*$ and $h(k) = h^*$, the closed-loop transfer function matches that of the reference model. Equation (47) is then transformed into space representation:

$$\epsilon(k+1) = A\epsilon(k) + bv(k) \tag{51}$$

$$\epsilon_1(k) = C^T\epsilon(k) + dv(k) \tag{52}$$

where

$$v(k) = \psi^T(k)\zeta(k) - k_0^*\alpha\zeta^T(k)\Gamma\zeta e_1(k) - k_0^* h(k)\xi(k) - k_0^*\beta\gamma\xi^2(k)e_1(k) \tag{53}$$

and

$$d + c^T(zI - A)^{-1}b = \text{ strictly positive real.}$$

Then, defining a Lyapunov function candidate $V(\epsilon(k), \psi(k))$ for this error system as

$$V(\epsilon(k), \psi(k)) = 2\epsilon^T(k)P\epsilon(k) + \psi^T(k)\Gamma^{-1}\psi(k) + h^T(k)\gamma^{-1}h \tag{54}$$

Table 1 Simulation Results of the Effect of β-term

	Adaptation gain		Quadratic term		Result 0 = stable
	Γ	γ	α	β	X = unstable
#1	1	1	0.1	0	X
#2	1	1	0.2	0	X
#3	1	1	0.41	0	X
#4	1	1	0.45	0	0
#5	1	1	0.48	0	0
#6	1	1	0.41	0.7	0
#7	1	1	0.07	0.6	0
#8	100	100	0.07	0.6	0

where

$$P = P^T > 0 \tag{55}$$

it straightforwardly follows, via use of the Kalman-Yacubovich Lemma, that

$$\Delta V(k) = (1 - 2k_0^*\alpha)\zeta^T(k)\Gamma\zeta(k)e_1^2(k) + (1 - 2\beta)\gamma\xi^2(k)e_1^2(k) \tag{56}$$

It is clear by now to see the effect of the additional quadratic feedback signal, i.e., $\beta\gamma\xi^2(k)$, (referred to as β-term thereafter), on the stability. If the β-term is neglected, there is no guarantee that $\Delta V(k) < 0$: the sign of $\Delta V(k)$ depends upon the relative magnitude of the two signals $\zeta(k)$ and $\xi(k)$. Considering the definition of the $\xi(k)$ in Equation (34), $\xi(k)$ is essentially a derivative signal. Thus, at the steady state, $\xi(k) = 0$ and hence it does not affect stability. It is in the transient phase that the signal $\xi(k)$ affects the stability, especially when the magnitude of the derivative signal $\xi(k)$ is large, for example when a big command or big adaptation gain is used.

A simulation study was conducted to support this argument. The following plant and model are used:

$$G_p(s) = \frac{0.1}{s + 0.2} \tag{57}$$

$$G_m(s) = \frac{1}{s + 1} \tag{58}$$

with the sampling frequency of 5 Hz.

The plant is initially assumed to be

$$G_p(s)|_{t=0} = \frac{1}{s + 1} \tag{59}$$

In Table 1, various combinations of (Γ, γ) (adaptation gain) and (α, β) (quadratic feedback terms) are used for simulations and the stability of the system is examined. In cases #1 through #5, it is immediately noticed that the condition $\alpha > k_p/k_m$ 1/2 (= 0.054) in equation (45) does not guarantee stability if the β-term is neglected. Also, α has to be larger than 0.41 in order to compensate for the effect of ξ(k) signal in Lyapunov difference in equation (56). However, case #3 is stabilized by the addition of β-term as shown in case #6 and because of this β-term, α can be reduced to 0.07 in case #7 and adaptation gain can be increased to a larger value in case #8.

Experiments are also conducted to demonstrate the stabilizing effect of the β-term. In Fig. 9, the reference model is chosen with time constant of 2 seconds and the sampling time is 0.2 seconds. Initial plant parameters are given so that the resulting controller yields extremely poor performance without adaptation ($\Gamma = \gamma = 0$) (*a*), then the adaptation is turned on ($\Gamma = \gamma = 1$) with $\alpha = 2$, $\beta = 0$ (unstable) (*b*), β is increased to $\beta = 0.5$ (*c*), and $\beta = 20$ (*d*). It is clearly shown that the stabilization and performance improvement are achieved by the use of additional β-term. We will see excellent performance of the MRAC/NL algorithm more in the welding experiments that follow.

Experimental Results

In this section, the closed-loop control experiments for the GTA welding are presented. Three controllers: PI, STC with pole placement (STC/PP, and MRAC of Narendra and Lin (MRAC/NL) are implemented. Various disturbances such as welding velocity, thickness and arc length change are introduced to the process so that the process parameters change significantly and the performance of the three controllers is compared.

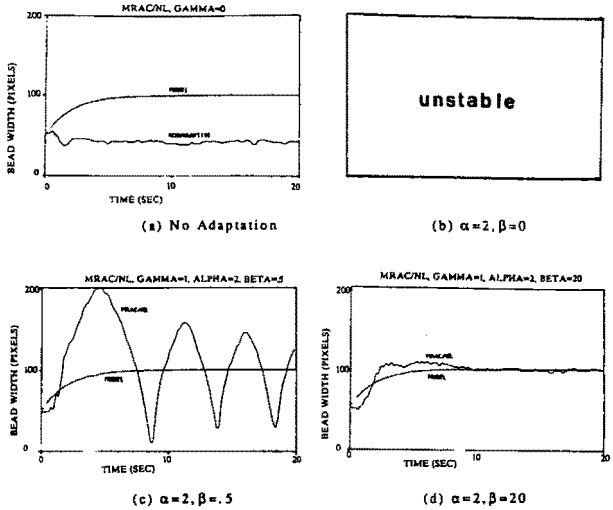

Fig. 9 Stabilizing effect of the β-term in MRAC/NL Algorithm for the GTA welding process

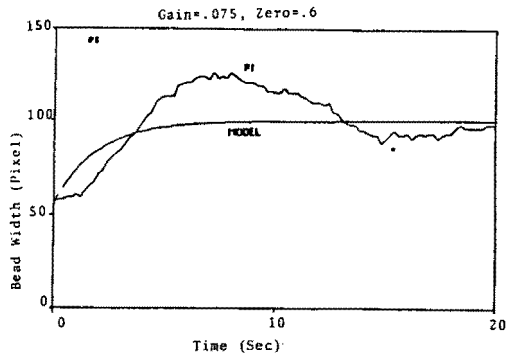

Fig. 10 Step response of the PI controller ($K_c = 0.075$, $c = 0.6$). (The output of the first order model is shown for comparison.)

Standard Conditions. Closed-loop step response tests under nominal conditions are conducted where the welding speed is 1.6 in/min, thickness is 0.109 in. and arc length is kept at 0.125 in. The desired (model) time constant is chosen as 2 and the sampling rate is 5 Hz.

For a linear controller, a Proportional and Integral (PI) controller was chosen to eliminate steady state error and to achieve reasonable transient response. The following standard structure is used:

$$\frac{u(z)}{e(z)} = \frac{K_c(z - c)}{z - 1} \tag{60}$$

Since we do not know the exact plant model nor the plant parameters, the controller gain K_c and zero c must be determined by trial and error tuning to achieve the desired response. The desired closed-loop specification in this case with the PI controller is to achieve zero steady state and to achieve minimal over-shoot while achieving as fast transient response as possible. Although it is impossible for the closed-loop system with PI control to follow the first-order reference model, the output of the first-order reference model used later for adaptive control systems is also shown in the same figure for a comparison. After careful tuning, the results of Fig. 10 were obtained, using a gain $K = 0.075$ and a zero located at 0.6. Since the nominal process model is first order, one may argue that further increase

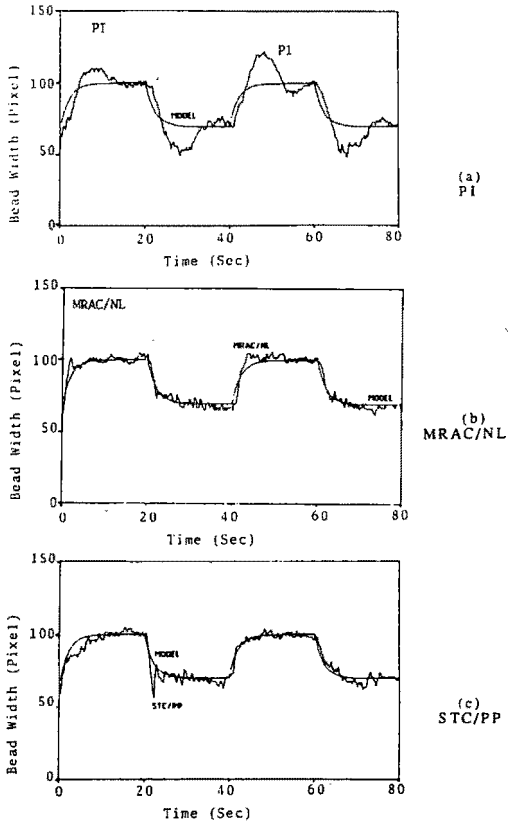

Fig. 11 Square wave following performance with three controllers under nominal conditions

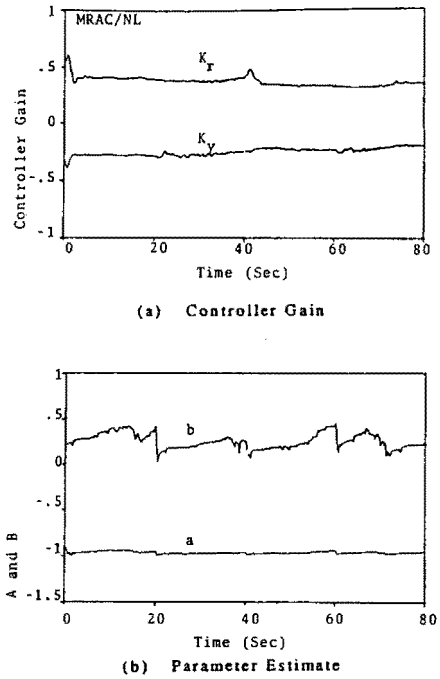

Fig. 12 Gain adapation in MRAC in Fig. 11(*b*) and parameter estimate in STC in Fig. 11(*c*)

of the controller gain will achieve faster, underdamped response. However, this is not the case because of both transport delay caused by the finite heat diffusion time from top to bottom of the weldment, and output noise. A high gain system will either result in instability due to this transport delay or be driven by the output noise.

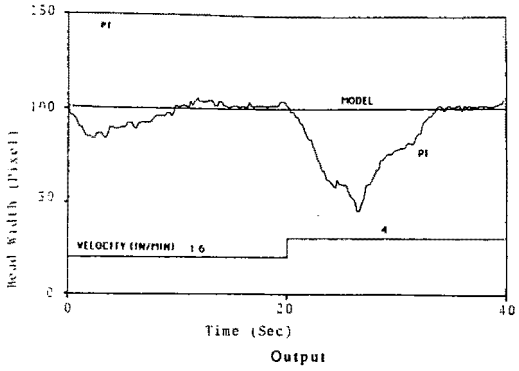

Fig. 13 PI under velocity change disturbance

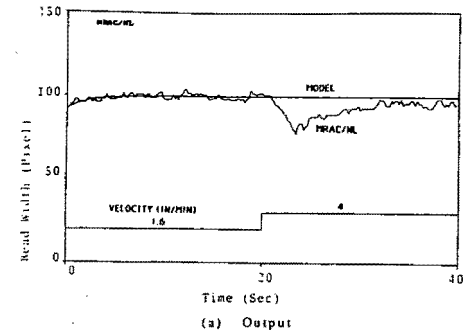

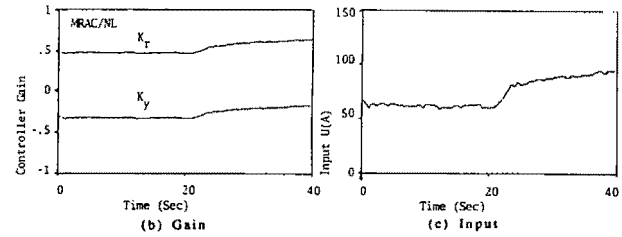

Fig. 14 MRAC/NL under velocity change disturbance

In Fig. 11, the command following performance for PI, MRAC/NL, and STC/PP under nominal conditions is shown. The initial plant parameter values for the latter two are $\tau_p = 6$s and $k_p = 6$. The step reference command is $r = 100$ (≈ 0.28 in) and $r = 70$ (≈ 0.196 in.). Other specific design parameters are $\Gamma = 1.0I$ and $\gamma = 1$ in. (*b*) and $P(0) = 0.5I$, $\lambda = 0.95$ in. (*c*). Both MRAC/NL and STC/PP clearly exhibited better performance than the linear PI controller in that the adaptive system does not require exact plant parameters but adjusts itself to attain the desired response. The gain adaptation and parameter estimates of these adaptive controllers are shown in Fig. 12. In the STC/PP algorithm, the estimate of $b(k)$ is not very smooth after each transient because the value of λ (forgetting factor) is too small. The effect of the forgetting factor in STC/PP and adaptation gains Γ and γ will be addressed later.

Torch Velocity Change as Disturbance. It was indicated earlier that the increase in torch velocity causes a decrease in both process gains and the time constant. Thus, if the torch velocity is changed during welding, the effect is reflected as a change in process dynamics, as well as in the process output as a pure disturbance. Therefore, the disturbance rejection property of the fixed PI control may not be satisfactory since it treats the disturbance as only a pure external disturbance. In Figs. 13–15, the torch velocity is increased stepwise at $t = 40$ sec. from 1.6 in/min to 4 in/min, and the sampling time is 5 Hz. Figure 13 demonstrates the performance with PI control.

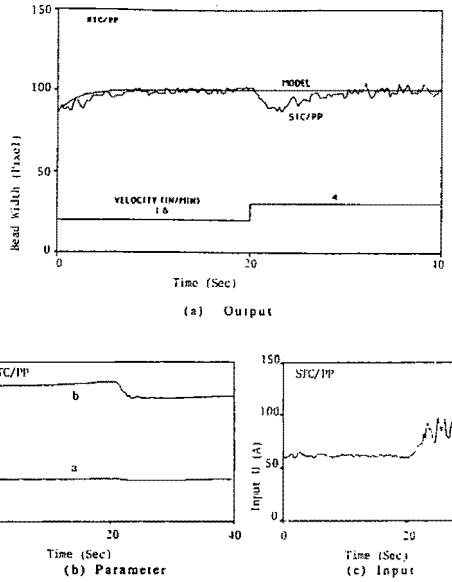

Fig. 15 STC/PP under velocity change disturbance

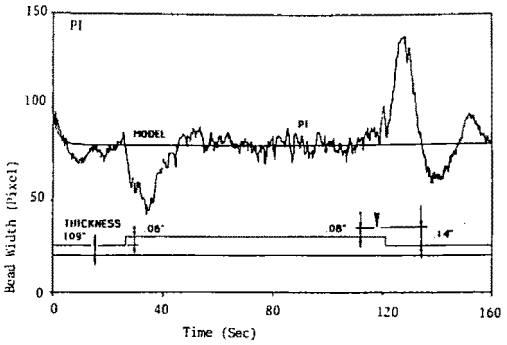

Fig. 16 PI under thickness change disturbance

Once the step velocity change occurs, the backbead width starts to decrease and after approximately 13 seconds the width is about 56 pixels (0.156 in.) below the command value, despite the controller's effort to increase the input current. In Fig. 14, the performance of MRAC/NL is shown where the width starts recovering only 6.7 seconds later the step velocity change occurs and the maximum deviation from the command value is only 22 pixels (0.061 in.) (60 percent reduction of the effort compared to PI). The gain is adjusted smoothly but reasonably quickly (Fig. 14(*b*) and the control input is shown in Fig. 14(*c*). The adaptation gains are $\Theta = I$ and $\gamma = 1$. Initial plant parameters are $\tau_p = 6$ seconds and $K_p = 6$.

Figure 15 depicts the response of the STC/PP algorithm. Again the significant adjustment and improved performance are observed. After about 7 seconds, the width losses only about 14 pixels (≈ 0.039 in.), even better than the previous MRAC case (74 percent reduction compared to PI). Plant parameter estimates are adjusted very quickly (Fig. 15(*b*). However, the estimate $b(k)$ decreases to a very small value which causes essentially high feedback as well as feedforward gain (refer to equation (19), resulting in a large high frequency component in the input (Fig. 15*c*). The same initial plant parameters as in the MRAC/NL (Fig. 14) are used. The forgetting factor and initial adaptation gain (covariance matrix) are $\lambda = 0.98$ and $P(0) = 0.1I$, respectively.

Thickness Change as Disturbance. Thickness change affects the process gain inversely according to the model in equation (7) and it has been verified by the experiments in Hardt, et al. (1985). We have also observed how the open-loop response is deteriorated by the thickness change in our specially prepared pipe shown in Fig. 5. In this experiment, the backbead width on this pipe is regulated by the same three controllers as before. The weld is made over the entire width of the attached sheet. We remark again that the disturbance involved in this preparation is primarily the thickness change but also the arc length change (shortened by the added thickness of 0.06 in.), different material properties and the possible existence of an air gap between two materials.

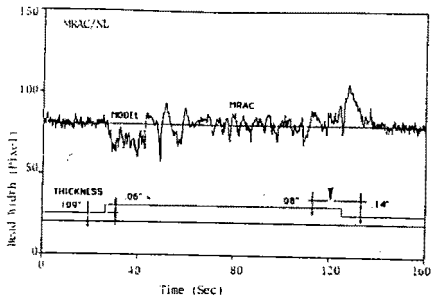

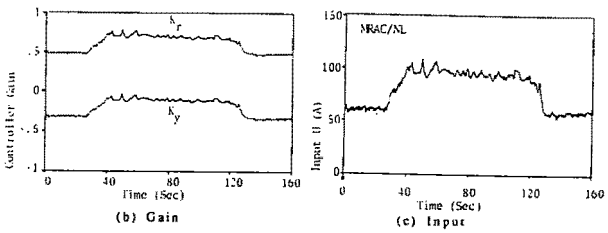

Fig. 17 MRAC/NL under thickness change disturbance

Figure 16 demonstrates the regulation performance by the PI control. After the torch enters the thicker region, the width keeps decreasing until it decreases by 37 pixels (0.103 in.). On the other hand, as the torch leaves the end edge of the thicker part, too much heat starts to melt the base material and the width increases by about 57 pixels (0.159 in.), and the regulation is oscillatory. The regulation or the disturbance rejection property of the PI controller is slow and poor as displayed in this figure. The torch velocity is 1.6 in/min, arc length is 0.08 in. over the attached sheet and the sampling frequency is 5 Hz. These are the parameters used in the next two figures.

Figure 17 shows the performance of the MRAC/NL. The bead width deviates from the target width as soon as the torch reaches the edge of the attached sheet but the controller gain is quickly adjusted so that the output width starts recovering after it has lost only 16 pixels (0.044 in.) 56 percent reduction of the error compared to PI). At the end of the attached sheet, the width starts increasing but again the controller gains are adjusted so that the maximum width is only 24 pixels (0.67 in.) above the target value (57 percent error reduction). The controller gains and control input are adjusted fast enough but smoothly as well. The adaptation gain was $\Gamma = 1.0I$ and $\gamma = 1.0$.

In Fig. 18, the performance of the STC/PP with pole placement is exhibited. The width deviation is kept within 15 pixels (0.042 in.) (59 percent error reduction compared to PI) at the entrance and 23 pixels (0.064 in.) (59 percent error reduction) at the exit, which is about the same as in the MRAC/NL, but the settling time is much faster than that of the MRAC/NL of the previous figure. This is because of high controller gain caused by a small estimated value of $b(k)$ as shown in the same figure.

Despite this excellent performance, it is necessary to examine Fig. 18 in more detail. At the edge of the attached sheet, the estimator sees the process gain decrease and thus $b(k)$ gets smaller while $a(k)$ is almost unchanged. After $t = 40$ seconds,

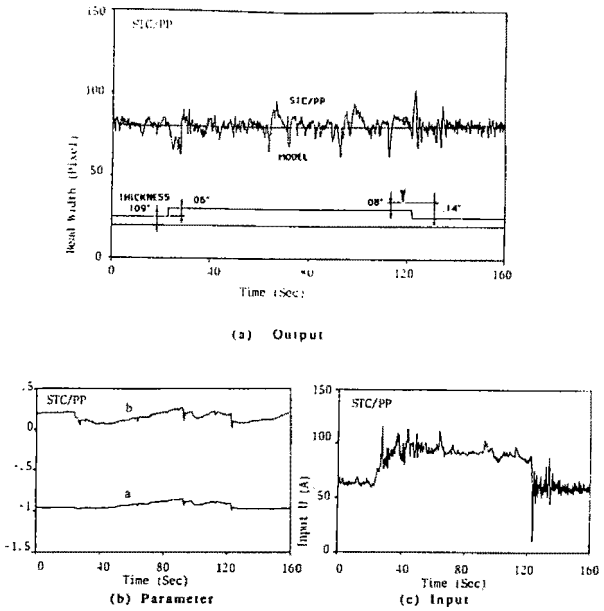

Fig. 18 STC/PP under thickness change disturbance

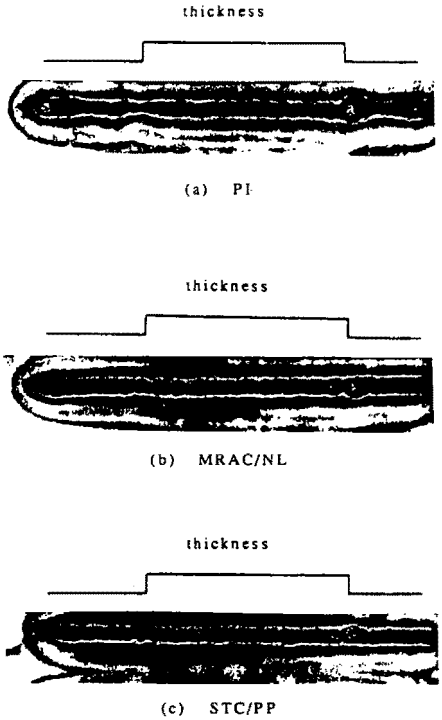

Fig. 19 Back side bead of three welding under thickness change disturbance

the parameter estimates start drifting because of a small forgetting factor ($\lambda = 0.98$) combined with output noise and a steady state situation. Then, at the other edge of the attached plate, the estimator recognizes that the process gain is increasing but at the same time constant has also increased because the whole area has been heated up (hence a smaller temperature gradient and an increased volume of the pool). Therefore, the estimate $a(k)$ is decreased (slower time constant) but the direction of $b(k)$ (increase or decrease) depends upon the ratio of the change in $a(k)$ and the change in k_p since k_p since $k_p(k) = b(k)/1 - a(k)$. In this case $b(k)$ at the exit edge has decreased. High frequency components in the input signal and, hence, in the output signal are simply caused by high controller gains driving the output noise. One of the drawbacks of the STC with pole placement, or most STCs in combination with other control laws, is that the updating of the controller gain involves the direct division by $b(k)$ or an equivalent $b(k)$ dependent quantity. The consequence of this is that the sensitivity of the closed-loop system to the parameter estimate increases dramatically when $b(k)$ becomes smaller. The initial covariance matrix was $P(0) = 0.02I$ in Fig. 18. The rest of the conditions are the same as in the previous two figures. Photographs of the final backbead by three controllers are shown in Fig. 19.

Discussion

The performance of the three controllers — the PI, the MRAC of Narendra and Lin, and the STC with pole placement — has been compared in three different situations: 1) consecutive step command (square wave) following; 2) step velocity change as disturbance; and 3) step thickness change as disturbance. In 1), even under the nominal conditions, the advantage of adaptive control was demonstrated in that it does not require the tedious fine tuning process required by PI control. Furthermore, with the PI control it is difficult to achieve both fast transient and small overshoot, whereas with the adaptive controller they are easily achieved even without knowing the process parameter values. In 2) and 3), the two adaptive controllers exhibit excellent adaptation and improved performance over PI control. In particular, the performance improvement of the adaptive controllers over the PI for the thickness change disturbance was dramatic. MRAC/NL showed, even in that case, smooth adaptation while retaining quick gain adjustment. However, the STC/PP exhibited a deadbeat-like response owing to a small estimate of $b(k)$ (essentially process gain) and an increased sensitivity of the controller gain to the parameter estimate.

The forgetting factor λ in equation (24) has an important effect on the performance of STC system. Note that the forgetting factor λ corresponds to remembering N numbers of most recent data,

$$\text{where } N = \frac{1}{(1-\lambda)} \tag{61}$$

Thus $\lambda = 0.98$ and $\lambda = 0.998$ correspond to $N = 50$ and $N = 500$, respectively. Therefore, a stepwise change in process dynamics, such as caused by thickness change, requires a reasonably small forgetting factor.

For example, if $\lambda = 1$ is used for the thickness change disturbance, we observed that the adaptation ability is lost by the end of the thick portion and the output and input signals are deteriorated. However, a small forgetting factor has other drawbacks. In Fig. 20, $\lambda = 0.005$ is used and the system is kept running at steady state for a long period of time. We observe a sudden burst of the system. This is explained as follows.

In the estimate algorithm of equation (21), the estimation gain or covariance matrix ($P(k)$ is proportional to parameter estimate covariance) defined by (Astrom (1983a);

$$P(k) = \sum_{i=1}^{k} \lambda^{k-i} \phi(i) \phi^T(i) \tag{62}$$

where $\phi(k)$ is a regressor vector. If $\lambda = 1$, then $P(k) - > 0$ as $K - > \infty$ and the adaption ability is lost. Consider the case where $\lambda < 1$ and the system stays at steady state. $P(k)$ is rewritten as (Astrom 1983a):

$$P(k) = [\phi(k)\phi^T(k) + \lambda P^{-1}(k-1)]^{-1} \tag{63}$$

At steady state, $\phi(k)$ is almost constant and the system is poorly excited. It is then shown after some algebra that the second term dominates equation (63), hence

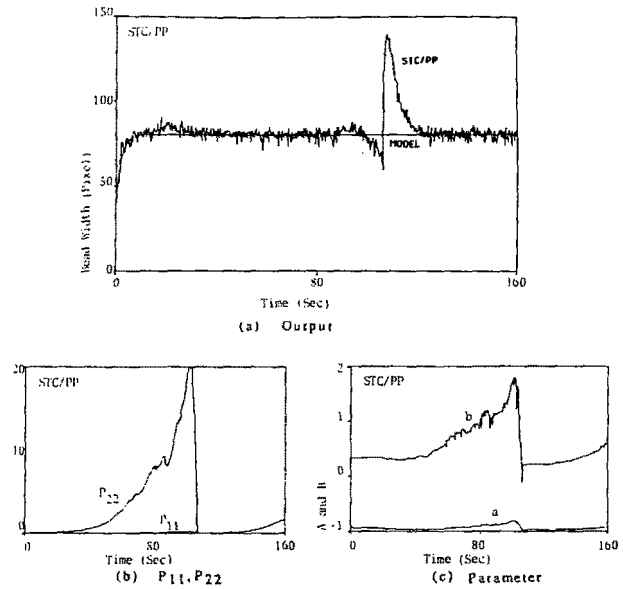

Fig. 20 STC/PP: long run under nominal condition with sampling frequency 5 HZ and $\lambda = 0.98$

$$P(k) = \frac{1}{\lambda} P(k-1) \tag{64}$$

and $P(k)$ grows exponentially (Astrom, 1983b). Figure 20(a) exhibits the diagonal elements of $P(k)$. Until about $t = 100$ seconds, the parameter keeps drifting because of the increasing $P(k)$ and existence of noise in the signal and the output starts to decrease (point T_1 in Fig. 20(a). Then an increase in the output error combined with the large $P(k)$ quickly recover the parameter estimates back to the normal value range. However, the estimation gain or covariance $P(k)$ has grown so large that the recovery is carried out with large bandwidth and, thus, the output jumps until the parameter estimates settle down. Such phenomena are not uncommon in STC applications and have been reported, for example, in Fortescue et al. (1981) and Kershenbaum and Fortescue [1981] as a sudden "blow-up" after a period of good regulation.

Parameter Drift. A similar long running test is conducted with the MRAC/NL and parameter drift is not observed at all. The welding conditions are the same as in the STC experiments with a sampling frequency of 5 Hz. in equation (61), the signal $\xi(k)$ vanishes at the steady state, hence

$$e_1(k) = \frac{e(k)}{1 + \alpha \zeta^T(k) \Gamma \zeta(k)} \tag{65}$$

We have seen that in the transient phase of the system response the quadratic term took the normalizing role of the adaptation and now at the steady state the α-term becomes dominant. The gain adjustment mechanism of equation (39) is expressed by

$$\phi(k+1) = \phi(k) - \Gamma \frac{e(k)}{1 + \alpha \zeta^T(k) \Gamma \zeta(k)} \zeta(k) \tag{66}$$

By comparison with the estimation mechanism of equation (21), restated here:

$$\theta(k+1) = \theta(k) + P_k \phi_k e(k) \tag{67}$$

it is easy to see the noise attenuation effect in the MRAC/NL algorithm.

Suppose at the steady state, the output noise $n(k)$ is dominant in the output error $e(k)$. Then in the estimation algorithm of equation (67), the second term on the RHS becomes:

$$\begin{aligned} \phi(k)e(k) &= \{y(k) + n(k)\} n(k) \\ &= n^2(k) + n(k) y(k) \end{aligned} \tag{68}$$

Thus the quadratic noise term $n^2(k)$ will cause drift encouraged by the growth in the covariance $P(k)$ aforementioned. On the other hand, in the adaptation mechanisms of the MRAC/NL of equation (65), two attenuation effects exist: an attenuation of the noise in the output error $e(k)$ by the α-term and an attenuation of the noise in the output $y(k)$ by the proper choice of the filter $L^{-1}(z)$. In our design, $L^{-1}(z)$ is chosen as $L^{-1}(z) = G_m(z)$ with the bandwidth of 0.5 rad/second, enough below the dominant noise range. Thus, MRAC/NL has inherent attenuation and filtering effects within the adaptation mechanism itself.

The final remarks on the experimental results are the comments on the adaptation gain in the MRAC/NL. The adaptation gains Γ and γ in equations (39) and (40) do not affect the speed of adaptation significantly since they also appear in the denominator in $e_1(k)$ as a normalization factor. This is also verified in the velocity change disturbance experiments using $\Gamma = \gamma = I$, 5I and 20I. In most experiments $\Gamma = \gamma = I$ is used unless otherwise specified. The speed of adaptation is rather affected by the value of α and the β. The smaller the α and the β are, the faster the adaptation speed but at the same time, the more oscillatory the system. With the same velocity change disturbance experiments, the effect of α is examined by changing the α from 2.0 to 1.0 and 0.5. The system gets oscillatory with $\alpha = 1.0$ and unstable with $\alpha = 0.5$. In most experiments, the α and the β are set to 2.0 and 1.0, respectively.

Conclusions

This paper contributes a demonstration of the application of adaptive control theory to the GTA welding process. The control system design essentially utilized the first order model with variable plant parameters derived in Hardt et al. (1985). Step response tests demonstrated that parameters responsible for the nonlinear nature of the process depend heavily on operating condition including torch velocity, arc length, input magnitude, input direction, and the material properties of the different batches. This dependence suggested the need for an adaptive compensation scheme.

Two algorithms have been chosen as the representative adaptive control algorithms: the MRAC developed by Narendra and Lin (MRAC/NL) and the STC with pole placement (STC/PP). Scrutiny of the former algorithm suggested the need for an additional quadratic term (β-term) to enhance nominal stability through Lyapunov analysis. Both simulation and experiment revealed the dramatic effect of the β-term.

The performance of the adaptive controllers was compared to the performance of the PI controller in three situations: (1) under the nominal conditions; (2) under conditions of step torch-velocity change; and (3) under conditions of step thickness change. In case (1), the two adaptive controllers showed excellent transient response while the PI controller exhibited more overshoot and slower response even after a tedious tuning process. In cases (2) and (3), both adaptive controllers greatly improved disturbances rejection. The response of the MRAC/NL to a thickness change was especially impressive, adjusting the controller gain smoothly, yet quickly. However, the STC/PP algorithm exhibited a response similar to the effect of a dead beat controller. This was partly due to the increased sensitivity of the controller gain to the parameter estimates.

Analysis showed that the two quadratic terms in the adaptation mechanism of MRAC/NL result in a normalizing effect on the generalized error signal, hence allowing the MRAC/NL controller to achieve a constant adaptation bandwidth. In particular, the normalizing effect of the β-term is significant in the transient phase of responses. Although the STC/PP algorithm possesses a similar normalization factor as well represented by the regressor vector, it does not possess an equivalent to the β-term. Further, the normalizing effect

of the regressor vector becomes less effective when the estimation gain $P(k)$ grows under steady state with a forgetting factor less than unity.

Also in contrast to the STC/PP, the adaptation mechanism in the MRAC/NL algorithm filters out the output noise. Because of this inherent filtering effect, the MRAC/NL did not exhibit any drift under steady state, whereas in the STC/PP the choice of a forgetting factor less than unity resulted in covariance growth under steady-state conditions. This covariance growth, combined with the lack of noise filtering, caused parameter drift resulting, in the worst observed case, in a sudden output burst.

The primary purpose of an adaptive control system is to maintain a constant closed-loop bandwidth despite the variations in process dynamics. The controller should accomplish this by means of adjusting the controller bandwidth without altering the "adaptation bandwidth." The adaptation bandwidth" should never vary. It should be insensitive to all operating conditions, including command magnitude and noise/disturbance. The adaptation mechanisms should include effective normalization factors within the mechanism itself, and MRAC/NL does, so that it is capable of controlling the "adaptation bandwidth." The adaptation mechanisms also should function to filter noise as in MRAC/NL in order to control the frequency content of the signal used in the adaptation mechanism.

We have not observed instability of drift when using the MRAC/NL algorithm. Still, since certain algorithms such as the STC/PP are more likely to suffer from parameter drift, it is a good idea to have a third loop, namely a supervisory loop, which detects the poor excitation situations such as occurred in the steady state.

References

Astrom, K. J., and Wittenmark, B., 1984, *Computer Controlled Systems*, Prentice-Hall, N.J.

Astrom, K. J., and Wittenmark, B., 1980, "Self Tuning Controllers Based on Pole-Zero Placement," *IEEE Proc.*, Vol. 127, Pt. D., No. 3, May.

Astrom, K. J., 1983a, "Theory and Application of Adaptive Control — A Survey," *Automatica*, Vol. 19, No. 5, Nov., p. 471

Astrom, K. J., 1983b, "Analysis of Rohrs Counterexample to Adaptive Control," *Proc. 22nd IEEE Conf. Decision Control*, San Antonio, TX, Dec., p. 982.

Bennett, A. P., and Smith, C. J., 1976, "Improving the Consistency of Weld Penetration by Feedback Control," *Welding Institute Conference Proceedings: Fabrication and Reliability of Welded Process Plant*, p. 13.

Cegrell, T., and Hedqvist, T., 1975, "Successful Adaptive Control of Paper Machines," *Automatica*, Vol. 11, p. 53.

Clarke, D. W., and Gawthrop, P. J., 1981, "Implementation and Application of Microprocessor-Based Self-Tuners," *Automatica*, Vol. 17, No. 1, p. 233.

Desrochers, A. A., 1981, "Intelligent Adaptive Control Strategies for Hot Steel Rolling Mills," *Proceedings of the Workshop on Applications of Adaptive Systems Theory*, Yale University, p. 125.

Doumanidis, C. C., and Hardt, D., 1988, "Multivariable Adaptive Control of Thermal Properties During Welding," ASME JOURNAL OF DYNAMIC SYSTEMS, MEASUREMENT AND CONTROL, May.

Egardt, B., 1980, "Unification of Some Discrete Time Adaptive Control Schemes," *IEEE Trans. A. C.*, Vol. AC-25, No. 4, Aug.

Finney, J. M., De Pennington, A., Bloor, M. S., and Gill, G. S., 1985, "A Pole Assignment Controller for an Electrohydraulic Cylinder Drive," JOURNAL OF DYNAMIC SYSTEMS, MEASUREMENT, AND CONTROL, Vol. 107, p.

Fortescue, T. R., Kershenbaum, L. S., and Ydstie, B. E., 1981, "Implementation of Self Tuning Regulators with Variable Forgetting Factors," *Automatica*, Vol. 17, No. 6, p. 831.

General Electric PN-2304 Optomation II Operating Manual, GE, Dec., 1981.

Goodwin, G. C., Ramadge, D. J., and Caines, P. E., 1980, "Discrete Time Multivariable Adaptive Control," *IEEE Trans. A. C.*, Vol. AC-25, No. 3, June.

Hardt, D. E., Garlow, D. A., and Weinert, J. B., 1985, "A Model of Full Penetration Arc-Welding for Control System Design," JOURNAL OF DYNAMIC SYSTEMS, MEASUREMENT AND CONTROL, Vol. 107, Mar.

Kershenbaum, L. S., and Fortescue, T. R., 1981, "Implementation of On-Line Control in Chemical Process Plants," *Automatica*, Vol. 17, No. 6, p. 777.

Kureishi, M., 1980, "Correlation Among Parameters Affecting on the Formation of Penetration Beads," *Yosetsu Gakkaishi*, Vol. 49, p. 17 (in Japanese).

Kurz, H., Isermann, R., and Schmann, R., 1980, "Experimental Comparison and Application of Various Parameter-Adaptive Control Algorithms," *Automatica*, Vol. 16, p. 1174.

Landau, Y. D., 1979, *Adaptive Control, The Model Reference Approach*, Marcel Dekker Inc., N.Y.

Leinonen, J. I., 1985, "Cast-to-Cast Variations in GTA Weld Penetration of Austentic Stainless Steels," *Welding Research: the State of the Art*, Conference Proceedings, Edited by Nippes, E. F., and J. B. Dorren, ASM, Oct.

Mills, G. S., 1979, "Fundamental Mechanisms of Penetration in GTA Welding," *Welding Journal*, Jan. P. 21-s.

Monopoli, R. V., 1974, "Model Reference Adaptive Control with an Augmented Error Signal," *IEEE Trans. A. C.* Vol. AC-19, No. 5, Oct.

Narendra, K. S., and Valavani, L. S., 1978, "Stable Adaptive Controller Design-Direct Control," *IEEE. Trans. A. C.*, Vol. AC-23, No. 4, Aug.

Narendra, K. S., and Lin, Y., 1980, "Stable Discrete Adaptive Control," *IEEE Trans. A. C.*, Vol. AC-25, No. 3, June.

Oshima, K., 1987, "Digital Control of the Pool Area in a Pulsed MIG Welding by the Use of CCD Camera," *Trans. IRR JAPAN*, Vol. 107-D, No. 9, p. 1159 (in Japanese).

Rohrs, C. E., 1982, *Adaptive Control in the Presence of Unmodeled Dynamics*, Ph.D. thesis, MIT.

Smith, C. J., 1974, "Self-Adaptive Control of Penetration in a Tungsten Inert Gas Weld," *Advances in Welding Processes*, Harrogate, Welding Institute Conference, p. 272.

Vroman, A. R., and Brandt, H., 1976, "Feedback Control of GTA Welding Using Puddle Width Measurement," *Welding Journal*, Sept. p. 742.

Walsh, D. W., and Savage, W. F., 1985, "Technical Note: Autogenous GTA Weldments-Bead Geometry Variations Due to Minor Elements," Welding Journal, Feb. p. 59-s.